Increased Bone Formation and Bone Mass Induced by Sclerostin Antibody Is Not Affected by Pretreatment or Cotreatment with Alendronate in Osteopenic, Ovariectomized Rats

Xiaodong Li, Michael S. Ominsky, Kelly S. Warmington, Qing-Tian Niu, Franklin J. Asuncion, Mauricio Barrero,* Denise Dwyer, Mario Grisanti, Marina Stolina, Paul J. Kostenuik, William S. Simonet, Chris Paszty, and Hua Zhu Ke

Department of Metabolic Disorders, Amgen, Inc., Thousand Oaks, California 91320

Clinical studies have revealed a blunting of the bone anabolic effects of parathyroid hormone treatment in osteoporotic patients in the setting of pre- or cotreatment with the antiresorptive agent alendronate (ALN). Sclerostin monoclonal antibody (Scl-Ab) is currently under clinical investigation as a new potential anabolic therapy for postmenopausal osteoporosis. The purpose of these experiments was to examine the influence of pretreatment or cotreatment with ALN on the bone anabolic actions of Scl-Ab in ovariectomized (OVX) rats. Ten-month-old osteopenic OVX rats were treated with ALN or vehicle for 6 wk, before the start of Scl-Ab treatment. ALN-pretreated OVX rats were switched to Scl-Ab alone or to a combination of ALN and Scl-Ab for another 6 wk. Vehicle-pretreated OVX rats were switched to Scl-Ab or continued on vehicle to serve as controls. Scl-Ab treatment increased areal bone mineral density, volumetric bone mineral density, trabecular and cortical bone mass, and bone strength similarly in OVX rats pretreated with ALN or vehicle. Serum osteocalcin and bone formation rate on trabecular, endocortical, and periosteal surfaces responded similarly to Scl-Ab in ALN or vehicle-pretreated OVX rats. Furthermore, cotreatment with ALN did not have significant effects on the increased bone formation, bone mass, and bone strength induced by Scl-Ab in the OVX rats that were pretreated with ALN. These results indicate that the increases in bone formation, bone mass, and bone strength with Scl-Ab treatment were not affected by pre- or cotreatment with ALN in OVX rats with established osteopenia. **(*Endocrinology* 152: 3312–3322, 2011)**

Sclerostin, secreted primarily by osteocytes, is a key negative regulator of bone formation (1–6). Pharmacologic inhibition of sclerostin using a sclerostin monoclonal antibody (Scl-Ab) has been shown to increase bone formation, bone mass, and bone strength in several rodent models of osteopenia (7–10) and in gonad-intact, nonhuman primates (11). Scl-Ab treatment stimulates bone formation on trabecular, endocortical (Ec.), and periosteal surfaces (Ps.) in rats (7–9) and nonhuman primates (11). Scl-Ab is currently under clinical investigation as a potential anabolic therapy for postmenopausal osteoporosis and fracture healing. In healthy men and postmenopausal women, a single sc administration of Scl-Ab increased several bone formation markers and decreased the bone resorption marker, serum C-terminal telopeptide of type I collagen (CTx-1), leading to increases in bone mineral density (BMD) (12).

The changes in serum biomarkers induced by Scl-Ab differ from those reported for human parathyroid hormone (PTH) (1-34). In humans, PTH increased both bone formation and bone resorption markers (13). Because

ISSN Print 0013-7227 ISSN Online 1945-7170
Printed in U.S.A.

doi: 10.1210/en.2011-0252 Received March 4, 2011. Accepted June 13, 2011.
First Published Online July 5, 2011

* Deceased author.

Abbreviations: ALN, Alendronate; BFR, bone formation rate; BMD, bone mineral density; BS, bone surface; BV/TV, bone volume fraction; μCT, micro-computed tomography; CTx-1, C-terminal telopeptide of type I collagen; Ec., endocortical; LV5, 5th lumbar vertebra; MAR, mineral apposition rate; MS/BS, mineralizing surface; Oc.S/BS, osteoclast surface; OVX, ovariectomized; Ps., periosteal; PTH, parathyroid hormone; Scl-Ab, sclerostin monoclonal antibody; sham, sham operated; TRACP 5b, tartrate-resistant acid phosphatase form 5b; vBMD, volumetric BMD.

PTH stimulates both bone formation and bone resorption, it was hypothesized that its bone mass-building effects might be enhanced when combined with a bone resorption inhibitor. However, clinical studies have revealed that cotreatment with the bisphosphonate alendronate (ALN) reduced the anabolic response to PTH treatment in both postmenopausal women and elderly osteoporotic men (14–17). The dependence of this anabolic response on bone resorption may be related to the finding in human biopsies that PTH increases bone formation primarily as part of the bone remodeling cycle (18–20).

Bisphosphonates are widely used as pharmacotherapy for postmenopausal osteoporosis, glucocorticoid-induced osteoporosis, and male osteoporosis (13–15). Despite the positive effects of bisphosphonates on BMD and fracture risk, many bisphosphonate-treated patients may be considered for anabolic treatment if they are severely osteoporotic or have failed prior therapy (21). Therefore, the effects of PTH have also been examined in patients with prior bisphosphonate treatment. These results demonstrated that the PTH-mediated increases in BMD were lower in ALN-treated patients than treatment-naïve patients (22). Furthermore, this anabolic-blunting effect was reflected at the tissue level with lower bone formation rate (BFR) values in iliac crest biopsies from ALN-treated patients compared with treatment-naïve patients after 1 month of PTH treatment (23). These results were consistent with the observed blunting effects of combination therapy and the fact that continued suppression of bone resorption was evident years after ALN discontinuation (24).

In contrast, Scl-Ab markedly stimulated bone formation on the quiescent surface of trabecular bone in ovariectomized (OVX) rats and nonhuman primates, suggesting that the bone anabolic activities of Scl-Ab may be independent of bone resorption (25, 26). Therefore, we hypothesized that the bone anabolic activity of a Scl-Ab would not be reduced by either pretreatment or cotreatment with ALN and investigated the hypothesis in a rat model of postmenopausal osteoporosis.

Materials and Methods

Study design

Six- and one-half-month-old virgin female Sprague Dawley rats (Harlan, Indianapolis, IN) were sham operated (Sham) or OVX and left untreated for 3.5 months, allowing for the development of osteopenia. The rats were then subjected to two 6-wk treatment phases. The first treatment phase included vehicle or ALN treatment (Table 1). During the first treatment phase, sham rats were injected sc with vehicle (saline) and OVX rats were injected sc with either vehicle or ALN (28 μg/kg, twice weekly) for 6 wk. A subset of ALN-treated OVX rats, vehicle-treated OVX rats, and sham rats was necropsied at the end of the 6-wk period (n = 10 per group). During the second treatment phase from wk 6 to 12, vehicle-treated sham rats were continued on vehicle (n = 10), whereas vehicle-treated OVX rats were either continued on vehicle or switched to a Scl-Ab specifically designed for rat studies (Scl-AbIII; 25 mg/kg, sc, once weekly) (n = 10 per group). ALN-treated OVX rats were given either Scl-Ab alone or Scl-Ab plus ALN (n = 10 per group). The doses of Scl-Ab and ALN were the same as described above. Animals from the second treatment phase were necropsied at the end of wk 12. All animals were housed in filter-top cages with food and water *ad libitum* on a 12-h light, 12-h dark cycle. The protocol and procedures were approved by the Institutional Animal Care and Use Committee of Amgen, Inc.

TABLE 1. Experimental design

Groups (n = 10)	First 6 wk	Second 6 wk
Sham-Vehicle	Vehicle	N/A
OVX-Vehicle	Vehicle	N/A
OVX-ALN	ALN	N/A
Sham-Vehicle/Vehicle	Vehicle	Vehicle
OVX-Vehicle/Vehicle	Vehicle	Vehicle
OVX-Vehicle/Scl-Ab	Vehicle	Scl-Ab
OVX-ALN/Scl-Ab	ALN	Scl-Ab
OVX-ALN/ALN + Scl-Ab	ALN	ALN + Scl-Ab

During the first 6 wk, sham or OVX rats were treated with saline (vehicle) or ALN (28 μg/kg, sc, twice weekly) for 6 wk. After 6 wk of treatment, these rats were either necropsied or continued in the second 6 wk. During the second 6 wk, rats were given vehicle, a Scl-Ab (25 mg/kg, sc, once weekly), or ALN in combination with Scl-Ab. N/A, Not applicable.

Body weights were recorded, and areal BMD was determined *in vivo* by dual-energy x-ray absorptiometry (Hologic QDR 4500a; Hologic, Bedford, MA) before the initiation of treatment. These measurements were used to assign rats to groups, so that all groups had similar body weights and BMD values before the start of treatment. BMD was monitored after 3, 6, 9, and 12 wk of treatment. Morning blood samples were collected after rats were fasted overnight after 0, 3, 6, 9, and 12 wk of treatment. Rats were injected sc with calcein (10 mg/kg) at 14, 13, 4, and 3 d before necropsy. At necropsy, the third lumbar vertebra and the right tibia were collected from each rat for dynamic histomorphometry, and the 5th lumbar vertebra (LV5) was collected for micro-computed tomography (μCT) and biomechanical analysis. One rat in the sham group died after wk 6 and was excluded from the data analysis.

Bone densitometry

Areal BMD was determined *in vivo* in isoflurane-anesthetized rats by dual-energy x-ray absorptiometry as described previously (27). The regions of interest included the lumbar vertebrae (LV1–LV5) and the femur-tibia (entire femur and the proximal half of the tibia). Longitudinal BMD data are only reported for the rats that were necropsied at wk 12.

Serum osteocalcin, CTx-1, and tartrate-resistant acid phosphatase form 5b (TRACP 5b)

Rats were fasted overnight before morning blood collection. At 48 h after each dose of Scl-Ab, rats were warmed for 10–15 min, and whole blood (0.7 ml) was collected from the tail vein into a serum separator tube (Microtainer; Becton Dickinson, Franklin Lakes, NJ). Serum osteocalcin was measured using a rat

Osteocalcin single plex LINCOplex kit (RBN-31K-1OC; Millipore; St. Charles, MO). The serum CTx-1 was measured using a commercially available enzyme immunoassay kit (IDS, Fountain Hills, AZ). TRACP 5b was measured using a rat ELISA kit (IDS). Longitudinal biomarker data are only reported for the rats necropsied at wk 12.

μCT analysis

Volumetric bone mineral content, volumetric BMD (vBMD), and microarchitecture of the LV5 body were examined using a desktop μCT system (GE eXplore Locus SP; GE Healthcare, Schenectady, NY) as described previously (28). The whole, trabecular, and cortical regions within the central 70% of the LV5 (reconstructed to 18-μm voxel size) were examined using a threshold of 550 mg HA/cm^3.

Bone histomorphometric analysis

Undecalcified parasagittal 4-μm-thick sections of the third lumbar vertebral bodies and 6-μm-thick transverse sections of tibia at the tibiofibular junction were prepared as described previously (7). Vertebral body sections were either stained with modified Goldner's Trichrome for analysis of static parameters or left unstained for collection of fluorochrome-based data. Tibial shaft sections were left unstained for collection of both fluorochrome-based and static parameter data. Histomorphometric analyses were made using Osteomeasure bone analysis software (Osteometrics, Inc., Decatur, GA). The region of interest for lumbar vertebral body trabecular bone included all trabecular bone within the parasagittal section. Static and dynamic parameters were calculated and expressed according to published methods (29, 30).

Bone strength testing

A 4-mm vertebral body specimen with parallel ends was prepared from the LV5 using a diamond wire saw (Well Diamond Wire Saws, Inc., Norcross, GA) and compressed to failure at a rate of 3 mm/min using an MTS 858 Mini Bionix servohydraulic system (MTS Systems, Corp., Eden Prairie, MN). Maximum load, stiffness, and energy to maximum load were generated from the load-deformation curves. One rat was excluded from data analysis in the sham group necropsied at wk 6 due to unusual load-displacement curve.

Statistics

All results were expressed as the mean ± SEM. Data were evaluated at individual time points by one-way ANOVA followed by the Tukey-Kramer *post hoc* test, using GraphPad Prism software (version 5.01; GraphPad Software, Inc., San Diego, CA). A P value of less than 0.05 was used to identify significant differences between any two groups. For the serum osteocalcin data, the absolute changes from wk 6 to 9 in the Scl-Ab treatment groups were further compared as described above.

Results

Areal BMD

Osteopenia was evident at both the lumbar vertebrae and femur-tibia sites in OVX rats compared with age-matched sham controls before the initiation of treatment (Fig. 1, A and B). During the first 6 wk of treatment, minor loss of BMD was observed at the lumbar vertebrae but not at the femur-tibia in the OVX-vehicle groups. ALN treatment did not have a significant effect on areal BMD at either site when compared with vehicle-treated OVX rats (Fig. 1, A and B). Similar changes were observed in the groups necropsied at wk 6 (data not shown).

During the second 6 wk of treatment, no additional decreases in BMD were observed at either site in the OVX-Vehicle/Vehicle group. Weekly Scl-Ab treatment, whether in vehicle- or ALN-pretreated OVX rats, or in combination with ALN in ALN-pretreated OVX rats, significantly increased areal BMD at both sites after 3 wk and restored BMD to levels similar to the sham group at both sites by 6 wk. There were no significant differences in BMD at either site among the three Scl-Ab-treated OVX groups. Additionally, Scl-Ab treatment had no effect on body weight or uterine weight (data not shown). OVX rats had significantly greater body weight but lower uterine weight than sham controls at the end of the study (data not shown).

Serum TRACP 5b, CTx-1, and osteocalcin

There was no significant difference in TRACP 5b between the sham and OVX groups before the initiation of treatment (Fig. 1C). Serum osteocalcin tended to be elevated in the OVX rats compared with sham control rats throughout the first 9 wk of the treatment period (Fig. 1D). Serum TRACP 5b or osteocalcin did not differ significantly among the four OVX groups before the initiation of treatment.

ALN treatment significantly decreased serum TRACP 5b and osteocalcin at wk 3 and 6 compared with the OVX controls (Fig. 1, C and D). Serum TRACP 5b or osteocalcin at wk 6 in ALN-treated OVX rats was about half of the corresponding OVX-vehicle values. ALN tended to decrease serum CTx-1, but no significant difference was observed between ALN-treated groups and OVX controls (data not shown).

Serum TRACP 5b in the Vehicle/Scl-Ab transition group was significantly lower than the OVX controls at wk 12. Serum TRACP 5b remained significantly lower than OVX controls in the ALN/Scl-Ab or ALN/ALN + Scl-Ab groups after transition to Scl-Ab. There were no significant differences in serum TRACP 5b among the three groups treated with Scl-Ab. There were no significant effects of Scl-Ab treatment on CTx-1 at wk 9 and 12 (data not shown). After initiation of Scl-Ab dosing, the absolute increases in osteocalcin from wk 6 to 9 were similar in the three Scl-Ab treatment groups (Vehicle/Scl-

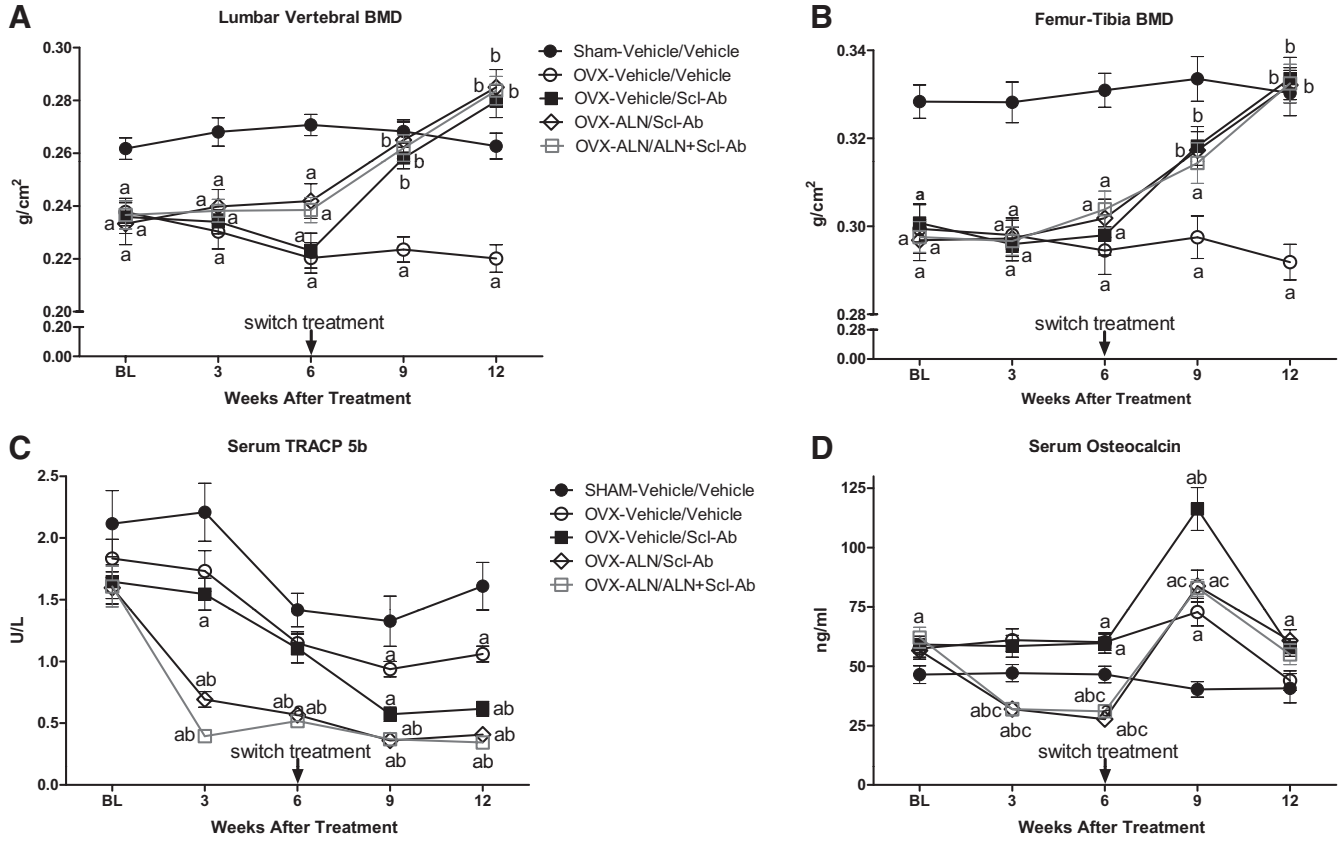

FIG. 1. Areal BMD and biochemical markers of bone turnover for the rats completing 12 wk of treatment. A, Areal BMD at lumbar spine. B, Areal BMD at femur-tibia. C, Serum TRACP 5b. D, Serum osteocalcin. BL, Baseline. *Arrow* indicates the time of switching the treatment from vehicle to Scl-Ab (Vehicle/Scl-Ab), ALN to Scl-Ab (ALN/Scl-Ab), or ALN to ALN + Scl-Ab (ALN/ALN + Scl-Ab). Data are expressed as the mean ± SEM for n = 10 per group with the exception of the sham group (n = 9). a, $P < 0.05$ compared with the age-matched sham group; b, $P < 0.05$ compared with the age-matched OVX + vehicle group; c, $P < 0.05$ compared with the OVX-Vehicle/Scl-Ab group.

Ab, 56.5 ± 6 ng/ml; ALN/Scl-Ab, 56.0 ± 6 ng/ml; ALN/ALN + Scl-Ab, 51.9 ± 3 ng/ml; $P = 0.8$ by ANOVA) (Fig. 1D). At wk 9 (3 wk after transition to Scl-Ab), total serum osteocalcin was significantly lower in the ALN-pretreated groups compared with the vehicle-pretreated group. This is likely due to the existing lower level of total serum osteocalcin induced by treatment with ALN at wk 6, before transition to Scl-Ab. From wk 9 to 12, serum osteocalcin declined in all OVX groups, with similar means among the Scl-Ab-treated groups at levels which tended to be greater than OVX-vehicle controls.

μCT analysis

Figure 2A shows the representative cross-sectional μCT images of the LV5 body, selected based on each group's median value for trabecular bone volume fraction (BV/TV) in the rats treated for 12 wk. Greater trabecular and cortical thickness is visible in all three groups treated with Scl-Ab.

μCT analysis confirmed that vehicle-treated OVX rats had significantly lower vBMD, cortical thickness, trabecular BV/TV, and trabecular thickness compared with the age-matched sham controls (Fig. 2, B–E) after the first 6 wk of treatment. The ALN-treated OVX group had significantly greater vBMD and trabecular BV/TV than vehicle-treated OVX controls but significantly lower vBMD and trabecular BV/TV compared with sham controls (Fig. 2, B and D). Trabecular number was significantly greater in the ALN-treated OVX group compared with vehicle-treated OVX controls (data not shown). Six weeks of ALN treatment had no significant effect on cortical and trabecular thickness (Fig. 2, C and E).

After 12 wk of treatment, the significant differences in vBMD, cortical thickness, trabecular BV/TV, and trabecular thickness between sham and OVX controls persisted. In the Vehicle/Scl-Ab transition group, Scl-Ab treatment significantly increased vBMD, trabecular BV/TV, cortical thickness, and trabecular thickness to levels similar to or above sham controls. Similar increases in vBMD, BV/TV, cortical thickness, and trabecular thickness were observed in the ALN/Scl-Ab and ALN/ALN + Scl-Ab groups. Trabecular number was significantly greater in ALN/ALN + Scl-Ab group compared with vehicle-treated OVX controls (data not shown), but there were no other significant differences among the groups (data not shown).

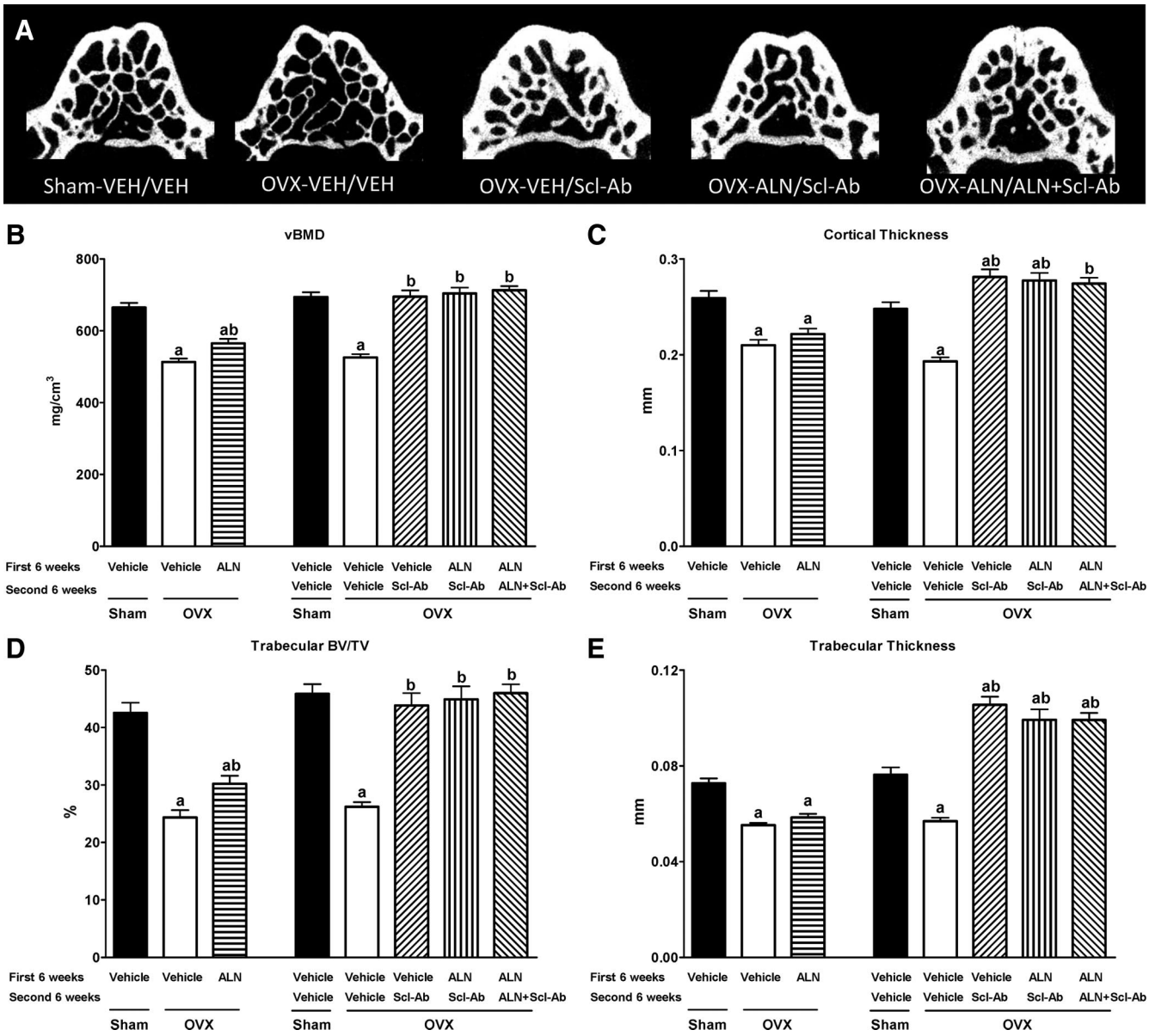

FIG. 2. Representative μCT images and selective μCT parameters of the LV5 body. A, Representative cross-sectional three-dimensional images of the LV5 body from each of the five groups treated for 12 wk. VEH, Vehicle. The images were selected based on each group's median value for BV/TV. A central 1-mm region was rendered for clarity. Greater trabecular and cortical thickness are visible in all three groups treated with Scl-Ab. B, vBMD of the LV5 body. C, Cortical thickness. D, Trabecular BV/TV. E, Trabecular thickness. Data represent mean ± SEM for 10 rats per group with the exception of the sham group (n = 9) taken down at wk 12. a, $P < 0.05$ compared with the respective sham control group; b, $P < 0.05$ compared with the respective OVX control group. The first three groups represent the rats taken down after 6 wk of treatment, and the five additional groups represent the rats taken down after 12 wk of treatment.

Histomorphometric analysis

Trabecular bone at the 3rd lumbar vertebral body

Static histomorphometric analysis confirmed that BV/TV and trabecular thickness were significantly higher in the Vehicle/Scl-Ab, ALN/Scl-Ab, and ALN/ALN + Scl-Ab groups than in vehicle-treated OVX controls at the end of the study (data not shown).

At wk 6, OVX rats had significantly greater mineralizing surface (MS/BS) and BFR/BS as compared with sham controls (Fig. 3, A and C). In OVX rats treated with ALN, significant decreases in MS/BS (−56%), mineral apposition rate (MAR) (−21%), and BFR/BS (−65%) were found when compared with vehicle-treated OVX rats (Fig. 3, A–C).

At wk 12, the difference in MS/BS and BFR/BS between sham and OVX controls was no longer significant. MAR was significantly greater in vehicle-treated OVX rats compared with sham controls. As expected, significant increases in MS/BS (+48%), MAR (+11%), and BFR/BS (+65%) were observed in the Vehicle/Scl-Ab transition group, compared with OVX-vehicle controls. Similar increases over OVX controls were observed in these param-

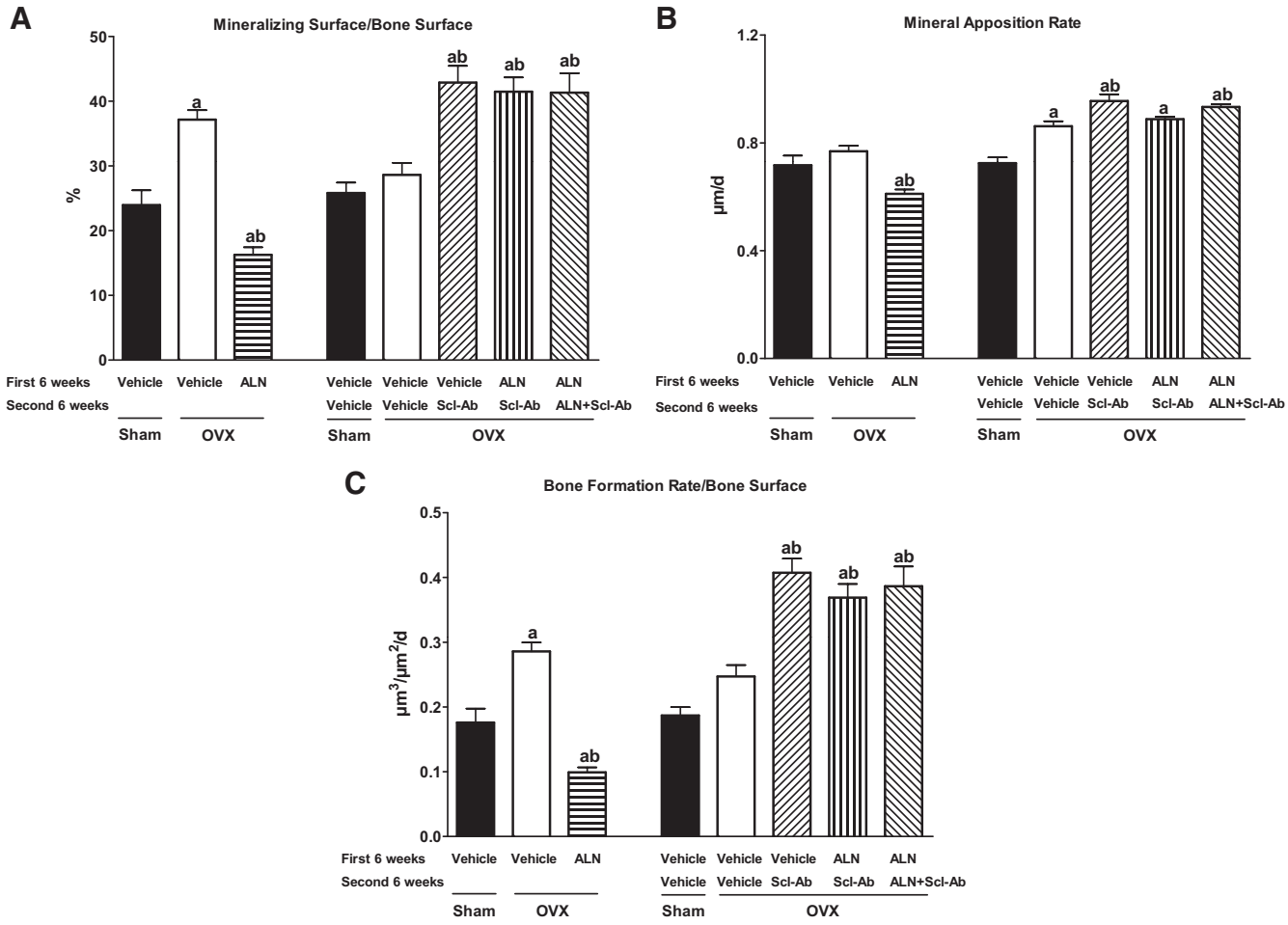

FIG. 3. Dynamic histomorphometric parameters at trabecular bone of 3rd lumbar vertebral body. A, MS/BS. B, MAR. C, BFR/BS. Data represent mean ± SEM for 10 rats per group with the exception of the sham group (n = 9) taken down at wk 12. a, $P < 0.05$ compared with the respective sham control group; b, $P < 0.05$ compared with the respective OVX control group. The first three groups represent the rats taken down after 6 wk of treatment, and the five additional groups represent the rats taken down after 12 wk of treatment.

eters in the ALN/Scl-Ab and ALN/ALN + Scl-Ab groups, with no significant differences found among the three Scl-Ab-treated groups. Osteoclast surface (Oc.S/BS) was similar in all three groups that received Scl-Ab and, in no case, differed from the values in vehicle-treated OVX rats. Mean ± SEM of Oc.S/BS (%) was 0.54 ± 0.07, 0.61 ± 0.03, and 0.66 ± 0.05, in the Vehicle/Scl-Ab, ALN/Scl-Ab, and ALN/ALN + Scl-Ab groups, respectively, whereas it was 0.42 ± 0.04 in vehicle-treated OVX rats (all $P > 0.05$ *vs.* OVX-vehicle/vehicle).

Cortical bone at the tibial shaft

OVX rats had significantly greater Ec. MS/BS and BFR/BS and nonsignificantly greater MAR than sham controls (Fig. 4, A–C) at wk 6. Six weeks of ALN treatment did not significantly change dynamic bone formation parameters on the Ec surface in OVX rats. Vehicle-treated OVX rats had slightly greater percent marrow cavity area than sham controls (Fig. 4D). ALN-treated OVX rats had significantly greater percent marrow cavity area than sham controls, likely reflecting the difference in original bone size between these two groups.

At wk 12, vehicle-treated OVX rats had significantly greater Ec. MS/BS and Ec. MAR and nonsignificantly greater BFR/BS than sham controls. These changes were associated with significantly greater percent marrow cavity area in vehicle-treated OVX rats as compared with age-matched sham controls (Fig. 4D). Similar to the findings from the dynamic histomorphometric analysis in trabecular bone of the vertebral body, significant and similar increases in Ec. MS/BS, MAR, and BFR/BS were found in all three groups that received Scl-Ab compared with OVX controls (Fig. 4, A–C). These changes were associated with significantly decreased percent marrow cavity area in all three groups that received Scl-Ab compared with vehicle-treated OVX rats (Fig. 4D). The percent marrow cavity area in the three Scl-Ab-treated groups was similar to that of sham controls ($P > 0.05$ *vs.* sham).

At wk 6, there were no significant differences in Ps. MS/BS, MAR, BFR/BS (Fig. 4, E–G), and cross-sectional

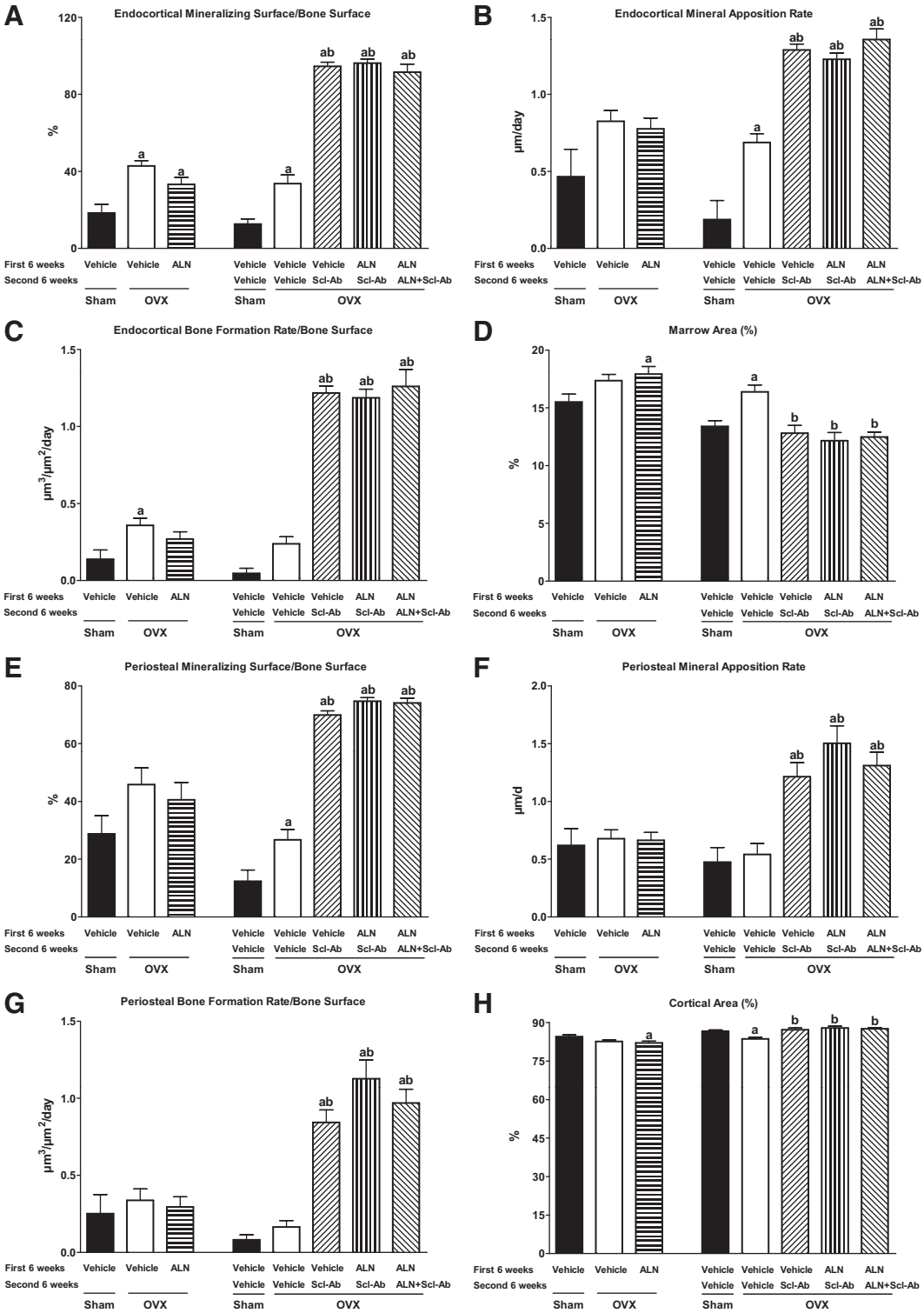

FIG. 4. Bone histomorphometric parameters at the Ec. and Ps. surface of the tibial shaft. A, Ec. MS/BS. B, Ec. MAR. C, Ec. BFR/BS. D, Percent marrow area. E, Ps. MS/BS. F, Ps. MAR. G, Ps. BFR/BS. H, Percent cortical area. Data represent mean ± SEM for 10 rats per group with the exception of the sham group (n = 9) taken down at wk 12. a, $P < 0.05$ compared with the respective sham control group; b, $P < 0.05$ compared with the respective OVX control group. The first three groups represent the rats taken down after 6 wk of treatment, and the five additional groups represent the rats taken down after 12 wk of treatment.

area (data not shown) among the sham and OVX controls and the ALN-treated OVX groups. At wk 12, significant and similar increases in MS/BS, MAR, and BFR/BS were observed in all three Scl-Ab groups compared with OVX controls. Consistent with findings in bone formation parameters, significant and similar increases in percent cor-

tical area were observed in all three Scl-Ab groups compared with OVX controls (Fig. 4H). There was no significant difference in cross-sectional area between the Vehicle/Scl-Ab, ALN/Scl-Ab, or ALN/ALN + Scl-Ab groups and OVX controls. However, the Vehicle/Scl-Ab group had significantly greater cross-sectional area than sham controls (data not shown).

Bone strength testing of the LV5

Destructive compression testing of the LV5 demonstrated that there were significant decreases in maximum load in the OVX-vehicle group when compared with sham controls at wk 6 (Fig. 5, A and B). ALN treatment alone had no significant effect on maximum load, stiffness, and energy to failure in OVX rats (Fig. 5, A–C).

At wk 12, the significant difference in maximum load persisted between sham and OVX controls. In addition, energy to failure was significantly lower in OVX rats compared with sham controls. In contrast, maximum load and stiffness in the three Scl-Ab groups were restored to equal levels that were significantly greater than those of both the OVX and sham controls (Fig. 5, A–C). Energy to failure in the three Scl-Ab groups was significantly greater than the OVX controls. No significant differences in maximum load, stiffness, and energy to failure were observed among the three groups that received Scl-Ab.

Discussion

Antiresorptive agents are commonly used to treat patients with osteoporosis. When additional increases in bone mass are required to further reduce fracture risk in these patients, bone anabolic agents may be considered as add-on or replacement therapy. The main purpose of the experiment described here was to investigate the effects of sclerostin inhibition alone or in combination with ALN on bone mass and bone formation in osteopenic OVX rats

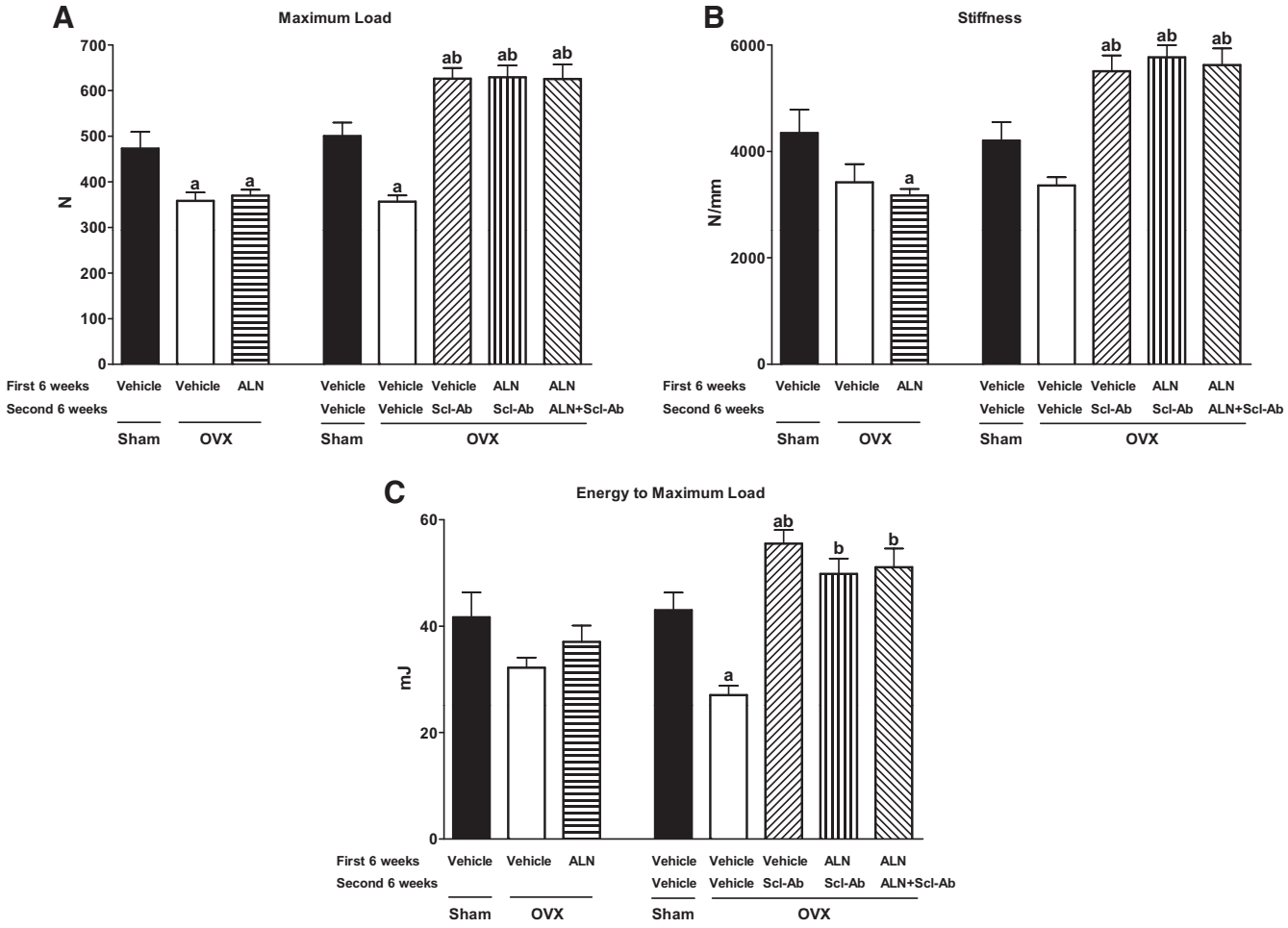

FIG. 5. Extrinsic bone strength parameters for the LV5. Vertebrae were obtained at the end of the treatment and tested to failure via a compression test. A, Maximum load. B, Stiffness. C, Energy to maximum load. Data represent mean ± SEM for 10 rats per group with the exception of the sham group (n = 9) taken down at wk 6 and the sham group (n = 9) taken down at wk 12. a, $P < 0.05$ compared with the respective sham control group; b, $P < 0.05$ compared with the respective OVX control group. The first three groups represent the rats taken down after 6 wk of treatment, and the five additional groups represent the rats taken down after 12 wk of treatment.

pretreated with ALN. The current rat experiment was intended to be a model for individuals with both estrogen deficiency-induced osteopenia and prior exposure to ALN. The dose of ALN in this study was the same as previously reported by others to fully inhibit loss of bone in the newly OVX adult rat (31–33). We found that weekly Scl-Ab treatment had similar anabolic effects in increasing bone formation, bone mass, and bone strength when administered either to OVX rats pretreated with vehicle or to OVX rats pretreated with ALN. Moreover, cotreatment with ALN had no significant effect on the ability of Scl-Ab to increase bone formation, bone mass, and bone strength. Within 6 wk, Scl-Ab treatment increased areal BMD at the lumbar vertebrae and femur-tibia regions to levels that matched or surpassed those in age-matched sham rats. As evidence that these bone mass rises were associated with increases in bone formation activity, Scl-Ab treatment not only increased serum osteocalcin but also increased key dynamic bone formation indices (MS/BS, MAR, and BFR/BS) at both trabecular surfaces and Ps. and Ec. surfaces of cortical bone similarly, in all treated groups. In all cases, the Scl-Ab-related increases in trabecular bone volume were associated with increased trabecular thickness, consistent with previous work with a Scl-Ab (7, 8). Although bone formation, bone mass, and bone strength were similar between the Scl-Ab alone group and the Scl-Ab in combination with ALN groups in this study, Scl-Ab in combination with an antiresorptive agent may offer an advantage over Scl-Ab alone, after discontinuation of treatment. This could be a topic of future investigation.

These experiments may also provide insight into the tissue level mechanisms by which Scl-Ab increases bone mass. The framework proposed for PTH, a bone anabolic agent, may be useful. PTH appears to exert its anabolic effects in the adult skeleton through two modes, one that increases bone formation without prior activation of resorption (modeling-based bone formation) (34–37) and a second that requires prior activation of resorption to increase bone formation, increasing the trabecular remodeling rate, and simultaneously creating positive bone balance at the bone multicellular level (remodeling-based bone formation) (38–40). Histology studies revealed that the majority of the anabolic effect of PTH treatment occurred on the remodeling-based bone forming surfaces in postmenopausal women (18–20). If the action of PTH is dependent on remodeling-based bone formation, then an antiremodeling agent like ALN may inhibit some of its anabolic action. In fact, this anabolic-blunting effect was reflected at the tissue level in lower BFR values in iliac crest biopsies from ALN-treated patients compared with treatment-naïve patients after 1 month of PTH treatment (23). The majority of small animal experiments indicated that cotreatment or prior treatment with bisphosphonates inhibited the ability of PTH to stimulate dynamic bone formation parameters in trabecular bone, despite a reasonable response in bone mass (41–44). These rodent data were consistent with human data that suggested a blunting effect of ALN treatment on PTH actions (14–17). However, a separate report has indicated that prior treatment with bisphosphonates had little effect on the response of bone formation to PTH treatment in OVX rats (33).

The current results in osteopenic, OVX rats, which demonstrate that Scl-Ab worked equally well in the presence or absence of efficacious doses of ALN, suggest that the anabolic effect of a Scl-Ab in OVX rats acts primarily through modeling-based bone formation. We have previously observed marked stimulation of bone formation on the quiescent surface of trabecular bone in Scl-Ab-treated OVX rats and nonhuman primates, indicating bone anabolic activities of Scl-Ab do not depend upon bone resorption (25, 26). These data provided supporting evidence for the current study. Whether these results will translate into humans will be the topic of future investigation.

The increase in anabolic activity with Scl-Ab was not associated with increases in the bone resorption marker, serum CTx-1, or in trabecular Oc.S/BS. Serum TRACP 5b, a marker of osteoclast number, was significantly lower in the Scl-Ab-treated group compared with vehicle-treated OVX controls. These results were supported by earlier studies of Scl-Ab administration in aged OVX rats, gonad-intact aged male rats, and gonad-intact female monkeys (7, 8, 11). A single administration of various doses of Scl-Ab was associated with dose-related increases in bone formation markers and decreases in serum CTx-1 in healthy men and postmenopausal women (12). These results point to a need for further investigation of the effect of Scl-Ab on bone resorption.

Despite similar BFR/BS among the three Scl-Ab groups on both trabecular and cortical surfaces, serum osteocalcin was significantly higher at wk 9 in the Vehicle/Scl-Ab group compared with the ALN/Scl-Ab group. The difference observed between these groups at wk 9 is equal to the difference between vehicle and ALN-treated groups at wk 3 or 6, likely reflecting the inhibition of ALN on bone formation before Scl-Ab treatment. The absolute increase in osteocalcin from wk 6 to 9 was similar in the three Scl-Ab treatment groups, indicating that the increased bone formation was not blocked by ALN pretreatment or/and cotreatment. The increased serum osteocalcin concentrations observed with Scl-Ab treatment appeared to return to baseline levels at wk 12 in all three Scl-Ab groups. However, histomorphometric analysis demonstrated that bone formation remained strongly stimulated on all bone surfaces in all three Scl-Ab groups at this time point. The

durability of the osteocalcin response to Scl-Ab therefore warrants further investigation.

In summary, weekly treatment with a Scl-Ab resulted in similar increases in bone formation, bone mass, and bone strength in OVX rats with or without ALN pretreatment. Moreover, cotreatment of Scl-Ab with ALN demonstrated equivalent efficacy as Scl-Ab alone in OVX rats pretreated with ALN. These results suggest that building bone via antibody-mediated sclerostin inhibition should be compatible with the historic and ongoing widespread use of bisphosphonates in osteoporosis therapy.

Acknowledgments

We thank Donald B. Kimmel, D.D.S., Ph.D., who provided thoughtful suggestions, comments, and editing of the manuscript and Michelle N. Bradley, Ph.D., of Amgen, Inc. who provided editorial support.

Parts of the manuscript were presented at the 30th Annual Meeting of the American Society for Bone and Mineral Research in Montreal, Canada, September 12–16, 2008, and at the 31st Annual Meeting of the American Society for Bone and Mineral Research in Denver, CO, September 11–15, 2009.

Address all correspondence and requests for reprints to: Xiaodong Li, M.D., Ph.D. Metabolic Disorders, 29-M-B, Amgen, Inc., One Amgen Center Drive, Thousand Oaks, California 91320. E-mail: xli@amgen.com; or Hua Zhu Ke, M.D. E-mail: hke@amgen.com.

This work was supported by Amgen, Inc. and UCB.

Disclosure Summary: All authors are Amgen, Inc. employees and own Amgen, Inc. stock and/or stock options.

References

1. **Brunkow ME, Gardner JC, Van Ness J, Paeper BW, Kovacevich BR, Proll S, Skonier JE, Zhao L, Sabo PJ, Fu Y, Alisch RS, Gillett L, Colbert T, Tacconi P, Galas D, Hamersma H, Beighton P, Mulligan J** 2001 Bone dysplasia sclerosteosis results from loss of the SOST gene product, a novel cystine knot-containing protein. Am J Hum Genet 68:577–589
2. **Balemans W, Ebeling M, Patel N, Van Hul E, Olson P, Dioszegi M, Lacza C, Wuyts W, Van Den Ende J, Willems P, Paes-Alves AF, Hill S, Bueno M, Ramos FJ, Tacconi P, Dikkers FG, Stratakis C, Lindpaintner K, Vickery B, Foernzler D, Van Hul W** 2001 Increased bone density in sclerosteosis is due to the deficiency of a novel secreted protein (SOST). Hum Mol Genet 10:537–543
3. **Winkler DG, Sutherland MK, Geoghegan JC, Yu C, Hayes T, Skonier JE, Shpektor D, Jonas M, Kovacevich BR, Staehling-Hampton K, Appleby M, Brunkow ME, Latham JA** 2003 Osteocyte control of bone formation via sclerostin, a novel BMP antagonist. EMBO J 22:6267–6276
4. **van Bezooijen RL, Roelen BA, Visser A, van der Wee-Pals L, de Wilt E, Karperien M, Hamersma H, Papapoulos SE, ten Dijke P, Löwik CW** 2004 Sclerostin is an osteocyte-expressed negative regulator of bone formation, but not a classical BMP antagonist. J Exp Med 199:805–814
5. **Poole KE, van Bezooijen RL, Loveridge N, Hamersma H, Papapoulos SE, Löwik CW, Reeve J** 2005 Sclerostin is a delayed secreted product of osteocytes that inhibits bone formation. FASEB J 19: 1842–1844
6. **Li X, Ominsky MS, Niu QT, Sun N, Daugherty B, D'Agostin D, Kurahara C, Gao Y, Cao J, Gong J, Asuncion F, Barrero M, Warmington K, Dwyer D, Stolina M, Morony S, Sarosi I, Kostenuik PJ, Lacey DL, Simonet WS, Ke HZ, Paszty C** 2008 Targeted deletion of the sclerostin gene in mice results in increased bone formation and bone strength. J Bone Miner Res 23:860–869
7. **Li X, Ominsky MS, Warmington KS, Morony S, Gong J, Cao J, Gao Y, Shalhoub V, Tipton B, Haldankar R, Chen Q, Winters A, Boone T, Geng Z, Niu QT, Ke HZ, Kostenuik PJ, Simonet WS, Lacey DL, Paszty C** 2009 Sclerostin antibody treatment increases bone formation, bone mass, and bone strength in a rat model of postmenopausal osteoporosis. J Bone Miner Res 24:578–588
8. **Li X, Warmington KS, Niu QT, Asuncion FJ, Barrero M, Grisanti M, Dwyer D, Stouch B, Thway TM, Stolina M, Ominsky MS, Kostenuik PJ, Simonet WS, Paszty C, Ke HZ** 2010 Inhibition of sclerostin by monoclonal antibody increases bone formation, bone mass, and bone strength in aged male rats. J Bone Miner Res 25:2371–2380
9. **Tian X, Jee WS, Li X, Paszty C, Ke HZ** 2011 Sclerostin antibody increases bone mass by stimulating bone formation and inhibiting bone resorption in a hindlimb-immobilization rat model. Bone 48: 197–201
10. **Eddleston A, Marenzana M, Moore AR, Stephens P, Muzylak M, Marshall D, Robinson MK** 2009 A short treatment with an antibody to sclerostin can inhibit bone loss in an ongoing model of colitis. J Bone Miner Res 24:1662–1671
11. **Ominsky MS, Vlasseros F, Jolette J, Smith SY, Stouch B, Doellgast G, Gong J, Gao Y, Cao J, Graham K, Tipton B, Cai J, Deshpande R, Zhou L, Hale MD, Lightwood DJ, Henry AJ, Popplewell AG, Moore AR, Robinson MK, Lacey DL, Simonet WS, Paszty C** 2010 Two doses of sclerostin antibody in cynomolgus monkeys increases bone formation, bone mineral density, and bone strength. J Bone Miner Res 25:948–959
12. **Padhi D, Jang G, Stouch B, Fang L, Posvar E** 2011 Single-dose, placebo-controlled, randomized study of AMG 785, a sclerostin monoclonal antibody. J Bone Miner Res 26:19–26
13. **Hodsman AB, Bauer DC, Dempster DW, Dian L, Hanley DA, Harris ST, Kendler DL, McClung MR, Miller PD, Olszynski WP, Orwoll E, Yuen CK** 2005 Parathyroid hormone and teriparatide for the treatment of osteoporosis: a review of the evidence and suggested guidelines for its use. Endocrine reviews 26:688–703
14. **Black DM, Greenspan SL, Ensrud KE, Palermo L, McGowan JA, Lang TF, Garnero P, Bouxsein ML, Bilezikian JP, Rosen CJ** 2003 The effects of parathyroid hormone and alendronate alone or in combination in postmenopausal osteoporosis. The New England journal of medicine 349:1207–1215
15. **Finkelstein JS, Hayes A, Hunzelman JL, Wyland JJ, Lee H, Neer RM** 2003 The effects of parathyroid hormone, alendronate, or both in men with osteoporosis. New Engl J Med 349:1216–1226
16. **Finkelstein JS, Leder BZ, Burnett SM, Wyland JJ, Lee H, de la Paz AV, Gibson K, Neer RM** 2006 Effects of teriparatide, alendronate, or both on bone turnover in osteoporotic men. J Clin Endocrinol Metab 91:2882–2887
17. **Finkelstein JS, Wyland JJ, Lee H, Neer RM** 2010 Effects of teriparatide, alendronate, or both in women with postmenopausal osteoporosis. J Clin Endocrinol Metab 95:1838–1845
18. **Lindsay R, Cosman F, Zhou H, Bostrom MP, Shen VW, Cruz JD, Nieves JW, Dempster DW** 2006 A novel tetracycline labeling schedule for longitudinal evaluation of the short-term effects of anabolic therapy with a single iliac crest bone biopsy: early actions of teriparatide. J Bone Miner Res 21:366–373
19. **Lindsay R, Zhou H, Cosman F, Nieves J, Dempster DW, Hodsman AB** 2007 Effects of a one-month treatment with PTH(1–34) on bone

formation on cancellous, endocortical, and periosteal surfaces of the human ilium. J Bone Miner Res 22:495–502
20. **Ma YL, Zeng Q, Donley DW, Ste-Marie LG, Gallagher JC, Dalsky GP, Marcus R, Eriksen EF** 2006 Teriparatide increases bone formation in modeling and remodeling osteons and enhances IGF-II immunoreactivity in postmenopausal women with osteoporosis. J Bone Miner Res 21:855–864
21. **Obermayer-Pietsch BM, Marin F, McCloskey EV, Hadji P, Farrerons J, Boonen S, Audran M, Barker C, Anastasilakis AD, Fraser WD, Nickelsen T** 2008 Effects of two years of daily teriparatide treatment on BMD in postmenopausal women with severe osteoporosis with and without prior antiresorptive treatment. J Bone Miner Res 23:1591–1600
22. **Boonen S, Marin F, Obermayer-Pietsch B, Simões ME, Barker C, Glass EV, Hadji P, Lyritis G, Oertel H, Nickelsen T, McCloskey EV** 2008 Effects of previous antiresorptive therapy on the bone mineral density response to two years of teriparatide treatment in postmenopausal women with osteoporosis. J Clin Endocrinol Metab 93:852–860
23. **Lindsay R, Cosman F, Zhou H, Bostrom MP, Nieves J, Dempster D** 2009 Early bone formaion response to teriparatide (TPTD) in subjects pre-treated with alendronate or residronate compared to treatment-naive subjects. J Bone Miner Res 24(S1):S213
24. **Black DM, Schwartz AV, Ensrud KE, Cauley JA, Levis S, Quandt SA, Satterfield S, Wallace RB, Bauer DC, Palermo L, Wehren LE, Lombardi A, Santora AC, Cummings SR** 2006 Effects of continuing or stopping alendronate after 5 years of treatment: the Fracture Intervention Trial Long-term Extension (FLEX): a randomized trial. JAMA 296:2927–2938
25. **Li X, Warmington KS, Niu Q-T, Grisanti M, Tan HL, Simonet WS, Kostenuik PJ, Paszty C, Ke HZ** 2007 Treatment with an anti-sclerostin antibody directly stimulates bone formation in a dose-dependent manner in ovariectomized rats with established osteopenia. J Bone Miner Res 22:S 65:1231
26. **Ominsky MS, Niu QT, Kurimoto P, Ke HZ** 2010 Tissue level mechanism of increased bone formation by sclerostin antibody in male cynomolgus monkeys. J Bone Miner Res 25:S 52:1174
27. **Kostenuik PJ, Capparelli C, Morony S, Adamu S, Shimamoto G, Shen V, Lacey DL, Dunstan CR** 2001 OPG and PTH-(1-34) have additive effects on bone density and mechanical strength in osteopenic ovariectomized rats. Endocrinology 142:4295–4304
28. **Ominsky MS, Li X, Asuncion FJ, Barrero M, Warmington KS, Dwyer D, Stolina M, Geng Z, Grisanti M, Tan HL, Corbin T, McCabe J, Simonet WS, Ke HZ, Kostenuik PJ** 2008 RANKL inhibition with osteoprotegerin increases bone strength by improving cortical and trabecular bone architecture in ovariectomized rats. J Bone Miner Res 23:672–682
29. **Parfitt AM, Drezner MK, Glorieux FH, Kanis JA, Malluche H, Meunier PJ, Ott SM, Recker RR** 1987 Bone histomorphometry: standardization of nomenclature, symbols, and units. Report of the ASBMR histomorphometry nomenclature committee. J Bone Miner Res 2:595–610
30. **Turner RT, Wakley GK, Hannon KS** 1990 Differential effects of androgens on cortical bone histomorphometry in gonadectomized male and female rats. J Orthop Res 8:612–617
31. **Seedor JG, Quartuccio HA, Thompson DD** 1991 The bisphosphonate alendronate (MK-217) inhibits bone loss due to ovariectomy in rats. J Bone Miner Res 6:339–346
32. **Toolan BC, Shea M, Myers ER, Borchers RE, Seedor JG, Quartuccio H, Rodan G, Hayes WC** 1992 Effects of 4-amino-1-hydroxybutylidene bisphosphonate on bone biomechanics in rats. J Bone Miner Res 7:1399–1406
33. **Ma YL, Bryant HU, Zeng Q, Schmidt A, Hoover J, Cole HW, Yao W, Jee WS, Sato M** 2003 New bone formation with teriparatide [human parathyroid hormone-(1–34)] is not retarded by long-term pretreatment with alendronate, estrogen, or raloxifene in ovariectomized rats. Endocrinology 144:2008–2015
34. **Hock JM, Hummert JR, Boyce R, Fonseca J, Raisz LG** 1989 Resorption is not essential for the stimulation of bone growth by hPTH-(1-34) in rats in vivo. J Bone Miner Res 4:449–458
35. **Hodsman AB, Steer BM** 1993 Early histomorphometric changes in response to parathyroid hormone therapy in osteoporosis: evidence for de novo bone formation on quiescent cancellous surfaces. Bone 14:523–527
36. **Dobnig H, Turner RT** 1995 Evidence that intermittent treatment with parathyroid hormone increases bone formation in adult rats by activation of bone lining cells. Endocrinology 136:3632–3638
37. **Nishida S, Yamaguchi A, Tanizawa T, Endo N, Mashiba T, Uchiyama Y, Suda T, Yoshiki S, Takahashi HE** 1994 Increased bone formation by intermittent parathyroid hormone administration is due to the stimulation of proliferation and differentiation of osteoprogenitor cells in bone marrow. Bone 15:717–723
38. **Bradbeer JN, Arlot ME, Meunier PJ, Reeve J** 1992 Treatment of osteoporosis with parathyroid peptide (hPTH 1-34) and oestrogen: increase in volumetric density of iliac cancellous bone may depend on reduced trabecular spacing as well as increased thickness of packets of newly formed bone. Clin Endocrinol 37:282–289
39. **Dempster DW** 1997 Exploiting and bypassing the bone remodeling cycle to optimize the treatment of osteoporosis. J Bone Miner Res 12:1152–1154
40. **Martin TJ** 2004 Does bone resorption inhibition affect the anabolic response to parathyroid hormone? Trends Endocrin Met 15:49–50
41. **Wronski TJ, Yen CF, Qi H, Dann LM** 1993 Parathyroid hormone is more effective than estrogen or bisphosphonates for restoration of lost bone mass in ovariectomized rats. Endocrinology 132:823–831
42. **Gasser JA, Kneissel M, Thomsen JS, Mosekilde L** 2000 PTH and interactions with bisphosphonates. J Musculoskelet Neural Interact 1:53–56
43. **Samadfam R, Xia Q, Goltzman D** 2007 Pretreatment with anticatabolic agents blunts but does not eliminate the skeletal anabolic response to parathyroid hormone in oophorectomized mice. Endocrinology 148:2778–2787
44. **Yao W, Su M, Zhang Q, Tian X, Setterberg RB, Blanton C, Lundy MW, Phipps R, Jee WS** 2007 Risedronate did not block the maximal anabolic effect of PTH in aged rats. Bone 41:813–819